THE EFFECTS OF HEIGHT AND PLAN ON THE ALONG- WIND RESPONSE OF STRUCTURES CONSIDERING WIND- SOIL- STRUCTURE INTERACTION

B. Shirkhanghah [a*], H. Eimani Kalehsar [b]

[a*] Department of Civil Engineering, University of Mohaghegh Ardabili, Ardabil, Iran, E-mail: behnam.shir@uma.ac.ir, Phone: +984533732100, Mobile: +989143548249, Fax: +984532524293
[b] Department of Civil Engineering, University of Mohaghegh Ardabili, Ardabil, Iran, e-mail: hek@uma.ac.ir, Phone: +9845 33513047, Mobile: +989143512509, Fax: +984533512910

Received: 09.06.2020 / Accepted: 11.07.2020/ Revised: 17.09.2020 / Available online: 15.12.020

DOI: 10.2478/jaes-2020-0025

KEY WORDS: Height, Plan, Along- Wind, Wind- Soil- Structure.

ABSTRACT:

The purpose of this study is to assess the effects of cross- section and slenderness on the dynamic response of high- rise buildings constructed on the coarse soil. In this work, the simulation of the wind and soil effects on the high-rise buildings are done numerically using the ABAQUS software. The wind-induced vibration of the building models is studied through Computational Fluid Dynamics (CFD) and Computational Structural Dynamics (CSD). Co- simulation is accepted for the transfer of loads from the fluid to the structural domain. The mechanical response of the soil system is modeled using direct method. Suitable contact elements for slippage and separation modeling between subsurface elements are also considered. Finally, fluid and structural responses are compared in terms of mean and root mean square values with laboratory results on the wide range of reduced velocities. It is concluded that height and cross- section of building affect the vibrational response of the building, and therefore the designer must carefully consider these factors in order to ensure that the design is safe.

1. INTRODUCTION

1.1 Coupled systems

Often, two or more physical systems interact with each other. In this case, the independent solution of each system is not possible without simultaneously solving other systems. Such systems are known as coupled systems. Such couplings may be weak or strong depending on the degree of interaction. Coupled systems are divided into two groups (Zienkiewicz & Taylor, 1998):

- Type I: This type includes issues in which coupling occurs at the interface between the domains through the imposed boundary conditions. Generally, domains describe different physical situations.
- Type II: This type includes issues which completely or partially overlap in different domains. In this research, the coupling is of the type I.

1.2 Previous studies

Wardlaw and Moss (1970), initially proposed standard modeling specifications for wind tunnel experiments of structures in which a simple CAARC model was used. Several experimental measurements were carried out on the CAARC building model during the 1970-1975 periods after the Wardlaw and Moss.

Melbourne (1980) provided a complete comparison between the results of the CAARC building, using these databases, including surface pressures and dynamic responses obtained at six research centers.

Numerical research on aerodynamics has been carried out since the early 1980s. One of the first papers was from Hirt et al. (1978). In this work, a finite difference model is proposed. Braun and Awruch (2009) conducted the numerical simulation of the aerodynamic and aero-elastic behavior of the CAARC building using a partitioned FSI technique. The damping effect of the structure and the locking phenomenon were shown (Braun & Awruch, 2009). In the recent paper, Huang et al. (2007) performed the aerodynamic analysis of the CAARC building model using numerical simulations. The aerodynamic coefficients and flow patterns around the building were determined using CFD commercial software. However, they found that the total cost of FSI simulations were relatively high. More work on computer simulation of wind effects on high-rise buildings may be found, for example, in Stathopoulos and Baskaran (1990).

The most common way to consider the effects of SSI is to model the subsystem with a set of visco- elastic elements (one for each degrees of freedom), whose coefficients of stiffness and damping are defined through equivalent springs and dampers (For example, (Harte et al., 2012; Kausel, 2010)).

* Corresponding author: Behnam Shirkhanghah, Department of Civil Engineering, University of Mohaghegh Ardabili, Ardabil, Iran, Phone: +984533732100, Mobile: +989143548249, Fax: +984532524293, e-mail: behnam.shir@uma.ac.ir

In some cases, this approach may be inaccurate. A completely powerful approach is used based on the finite element method to set up a precise model of the soil system in the near field bounded by artificial or infinite boundaries, while the linear elastic response of the far field model is used. In the near field, soil can be characterized by elastic or completely inelastic models (For example, Halabian & Naggar, 2002; Jeremic et al., 2009). This approach has many advantages.

1.3 Current study

In this research, the interaction of structures rested on soil subjected to wind with different speeds is investigated. The effect of various factors such as slenderness ratio and cross-sectional shape are investigated. In this numerical method, the natural non-uniform wind at the atmospheric boundary layer is modelled as smooth flow at the input. Then, the turbulent flow is simulated with the implicit large eddy Simulation (ILES) method, and the co-simulation scheme for the transfer of non-uniform loads from the fluid to the structural nodes is adopted. Aerodynamic damping is not considered. Infinite boundary conditions have been assigned to the numerical model for the simulation of free boundaries, and suitable contact elements for slippage and separating modelling between soil and footing are also considered. The critical velocity of the wind is computed in which the transverse displacement of the structure increases. The phenomenon of locking in structures is investigated and spectral diagrams are plotted for longitudinal responses.

The effect of wind- soil- structure interaction is investigated using ABAQUS finite element software, considering the linear behaviour of the soil and structure. The ABAQUS software is based on finite element and finite volume methods, which was first used by Clough in the 1960s. Its units provide the ability to model various complex shapes and analyse a variety of issues such as the dynamics of structures and fluids, and so on. One of its most powerful tools is ABAQUS /CFD. This software is the strongest software for the analysis of structure and fluid interaction. Due to its ease of use, its beautiful environment, its robust post-analysis abilities, this software has been at great attention. Geometric modelling is in Part module, definition of materials properties is in Material module, setting up problem defaults is in the Step module, production of mesh is in Mesh module, solving of problem in is Job module and observing of the results is in Visualization module (ABAQUS, 2012).

2. GOVERNING EQUATIONS OF FLUID-STRUCTURE INTERACTION

The governing equations of the fluid motion are the Navier-Stokes equations, mass equations, continuity and energy in the residual state that are solved by ABAQUS/CFD and the forces imposed on the structure are calculated. The equations governing the motion of a structure are momentum equations, the mass conservation principle and the material constitutive law for strain- stress measurements. These equations are also solved by the ABAQUS/Standard software and the displacements are calculated.

2.1 Simulation of fluid- structure interaction

The coupling scheme plays a major role in numerical simulation of the FSI. In the FSI analysis, mechanical balance and kinematic continuity must be satisfied on the interface between different physical territories, which are performed using numerical coupling algorithms. Coupling algorithms are categorized as continuous or partitioned (see Felippa et al. (2001), Zhang and Hisada (2004)), where the first, uses the united system of governing equations to analyze the FSI problem, and the latter leads to the independent solution of each subdomain in a successive method. In the CWE field, aero-elastic analysis is used to determine the effect of wind on structures, which mechanical and fluid forces are interacting significantly. Since continuous model is inefficient in the CWE issues, the partitioned model is used in this work.

2.2 Co- simulation boundaries

In this investigation, the interaction between domains is via a common physical interface, which data such as the pressure applied by the fluid to the structure or displacement of the structure due to the pressure of the fluid are transferred between the coupled analytical programs consecutively.

3. GOVERNING EQUATIONS OF SOIL- STRUCTURE INTERACTION

The structure-soil interaction system consists of two substructures: the structure and the soil. The equations governing the motion of soil and structure are also the dynamic equations of motion that are solved by the ABAQUS/Standard software.

3.1 Simulation of soil- structure interaction

The direct method of analysis, in which the entire structure-soil system is modeled in one step (without the need for separating of system into the superstructure and the substructure), can lead to more accurate modeling and analysis, but the most advanced program computer programs are required in this method. Since superposition hypothesis is not used, real and nonlinear analysis is possible in this case (Borja et al., 1994). Therefore, the direct method, which is better in modeling the complex nature of soil-structure interaction in dynamic analysis, was used in this study. ABAQUS Software was used in this study for numerical simulation of soil-structure interaction. This package can simulate complex problems requiring large computational RAM using the direct analysis method. A number of researchers (for example, Matinmanesh and Asheghabadi 2011, Chu and Truman 2004) used ABAQUS to investigate soil- structure interaction (Matinmanesh & Asheghabadi, 2011; Chu & Truman, 2004). The numerical modeling method for simulating structural and soil model, as well as contact surfaces and boundary conditions, are described below.

3.2 Contact surfaces

Contact elements are used to combine different mechanical properties of the soil and shallow footing, while any separation and slippage on the underlying soil during wind excitement are indicated. In order to analyse the structure-soil interaction in this study, surface-to-surface contact is defined. The master surface is the top level of soil and the slave surface is the bottom level of the footing.

4. INVESTIGATED PROBLEM

4.1 Structure

The standard model of the CAARC building is presented as the rectangular section with the flat roof and vertical walls (see Figure 1). The full dimensions of the building model are as: height (H = 180m); length (L = 30m); width (W = 45m). The dimensions of the model are scaled by 1/250 to be compared with tunnel measurements of the same scale. The structural damping ratio is 1%. The structure is discretized by 5 in 8 in 25 three-dimensional linear elastic brick elements. The total number of nodes and elements are 2220 and 2926, respectively. An average density of 160 kg/m3 for the whole building is assumed, as proposed by Melbourne (1980). Young's modulus is derived from the large number of numerical tests performed to calibrate this parameter based on the dynamic behaviour expected for the current building. The mechanical properties of the structure are shown in Table 1.

Specific Mass-ρ	160
Natural Frequency-n	0.2
Young Modulus-E	2.3e8
Poisson Ratio-ν	0.25
Damping Ratio-ζ	1%

Table 1. Mechnical properties of structure

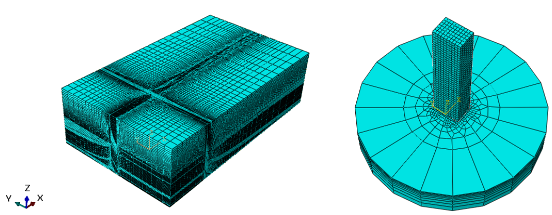

Figure 1. Mesh configuration for the CAARC building and wind flow

4.2 Fluid

The applied wind at the inlet is modelled using the power law equation as:

$$\frac{V(Z)}{V_H} = \left(\frac{Z}{H}\right)^{\alpha} \tag{1}$$

Where, $V(Z)$ is the wind speed at the height Z and V_H is the wind speed at top of the building, equal to 12.7m/s. The coefficient α is also the wind profile coefficient, which is 0.28 for open ground condition. Physical wind constants are shown in Table 2, which leads to the Reynolds number of *Re* =156575. The aero-elastic simulations were carried out in this paper, which holds the same Reynolds number in a wide range of wind speeds. A computational domain that is defined for the present simulations and the model location are shown also in Figure 1. Dimensions of the numerical wind tunnel are 28*L* in the *X* direction, 16*L* in the *Y* direction and 2*H* in the *Z* direction.

Specific Mass-ρ	1.25
Dynamic Viscosity-μ	1.825e-5
Reference Velocity (Inflow at Z=180)-V_H	12.7
Characteristic Dimension (Width)-W	0.18

Table 2. Mechnical properties of fluid

The mesh is composed of 497,000 octagonal elements and 519726 nodes, where the elements minimum height is about 1 mm, which is related to the elements in contact with the walls of the building. The height of the first elements near the walls are smaller than about $L/1000$, and the result of $y^+(\rho u y/\mu)$ is less than 5. The direction of the wind is along the x-axis towards the large building surface. Regular meshes are used for the prismatic hexahedral element in the fluid domain. The time step is fixed at Δt= 0.01s and the total physical time is t= 2s. The calculations took place at the supercomputer centre in Amirkabir University.

Although the response of wind to high-rise buildings typically results in asymmetry of the back flow separated from the lateral walls, the aero-elastic instability may occur when the natural frequency of the structure in the transverse direction is close to the shedding frequency of the vortices. The flow field is formed around the building, which causes more fluctuations in the transverse direction. At this stage, the mechanical frequency of the building controls the flow of the vortices. In the aero-elasticity, this phenomenon is known as locking. In order to obtain the reference speed for the flow field equivalent to the critical velocity, which results in the coordination between mechanical frequencies and a vortex shedding, the following relation is used:

$$St = \frac{f_v D}{V} \quad \rightarrow \quad V_{cr} = \frac{f_n D}{St} \tag{2}$$

Where St is the Strouhal number, f_v is the vortex shedding frequency, f_n is the natural frequency of the structure, and D is the characteristic dimension of the building in the transverse direction. According to the previous experimental work (e.g. Melbourne, 1980), the Strouhal number for the current problem is St =0.1.

4.3 Soil and footing

Rectangular concrete footing with dimensions of 40m in 50m, total height of 3.5 m and buried depth of 3.5 m, which is located on a hard 50-meter soil, classified according to Iranian standard as type 2. The soil density is 2160 kg/m^3. The properties of this soil are extracted from actual experiments in the site and in the laboratory and are shown in Table 3. It was assumed that the water level is below the footing level. The tangential behaviour of contact surfaces in the finite element model was used to model the classical Mohr- Coulomb model. In this simulation, the normal contact rigidity coefficient is equal to 1, and the maximum contact coefficient of friction is equal to 0.84. The total numbers of contact elements are 360.

Soil Properties	Value
Specific Mass	2160
Poisson's Ratio	0.3
Shear modulus	4160000
Angle of Friction	46.22
Flow Stress Ratio	0.788
Dilation Angle	0.1

Table 3. Soil properties

Extended Drucker-Prager model is used to model frictional materials such as soil and rock, and show pressure- dependent function, in which the material becomes stronger when the pressure rises. In order to achieve a reasonable scale model, a dynamic similarity between the model and the prototype should be used. The dynamic similarity provides conditions in which similar parts of the model and prototype experience the same pure forces. The main scaling coefficients are presented in Table 4. Using the geometric scale of 1/250, the diameter and depth of the cylindrical soil model are determined to be 0.6 m and 0.2 m, respectively. Other soil properties in the Drucker-Prager model after being scaled are shown in this table.

Mass Density	1	Time	$\lambda^{1/2}$
Force	λ^3	Frequency	$\lambda^{-1/2}$
Stiffness	λ^2	Length	λ
Modulus	λ	Stress	λ

Table 4. Scaling coefficients based on geometric scale factor

5. VERIFICATION

The pattern of wind pressure distribution on the surfaces of the CAARC standard tall building model is very complicated, and phenomena such as reverse flow and vortex shedding always occur. The contours of wind pressure coefficients are shown in Figure 2. The agreement of pressure distribution in the windward is very good with the predictions obtained by Huang et al. (2007). The results are more dispersed on the leeward.

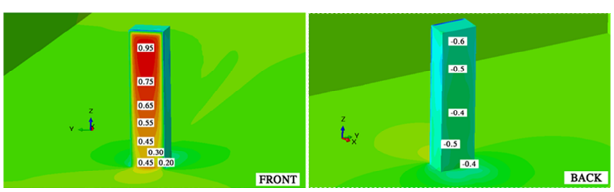

Figure 2. Mean pressure coefficient on the CAARC building front and back surfaces

6. AERO-ELASTIC ANALYSIS

The aero-elastic behaviour of the CAARC building model was investigated by analysing its structural response under five wind speeds in accordance with reduced velocities $V_r= V_H/nW=$ 2, 4, 6, 8, and 10. The time integration of the governing equations with the time step of $\Delta t= 0.005$ s is performed for all the simulations. Several other numerical simulations are also carried out in terms of building model with circular cross-section that its area is equal to the CAARC building and building model that its height is half of the CAARC building, in order to compare the effects of this parameter on the structural response (see Figure 3). The structural damping is not considered in these simulations.

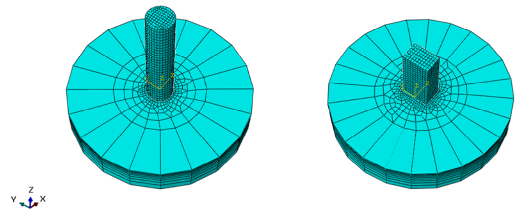

Figure 3. Mesh configuration for the circular and short building models

The results of simulation for CAARC building carried out without damping of the structure are given in Figure 4. As expected, the longitudinal displacement amplitude increases with increasing of wind speed, which also is confirmed for the mean longitudinal displacement. At $V_H/nW=2$ the response amplitude is constant, where the aerodynamic damping is very low. For the rest of the wind velocities, the longitudinal response gradually decreases because of dissipation effect of soil.

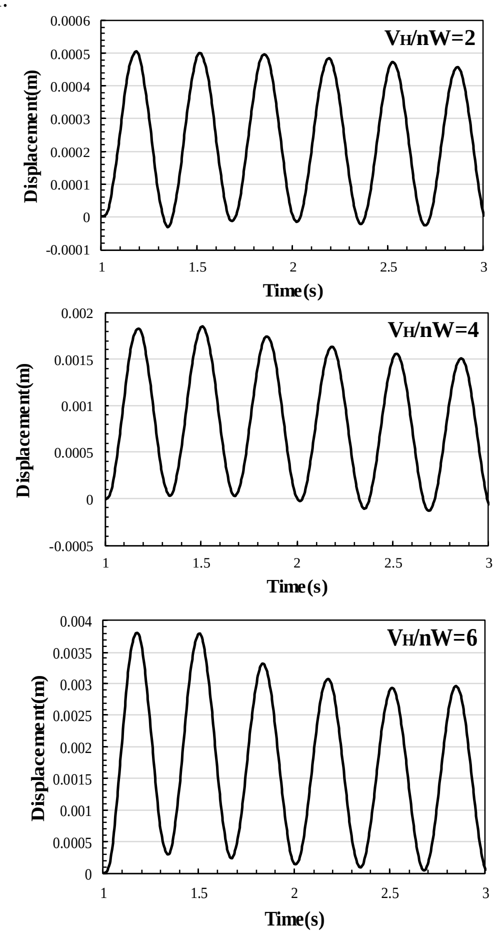

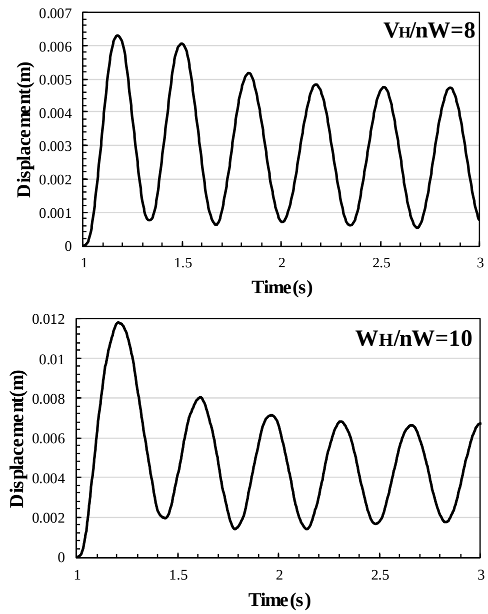

Figure 4. Time histories for along- wind displacements above the CAARC building for V_r= 2, 4, 6, 8 and 10

In the numerical simulation of the locking speed (V_H/nW= 10), a structural reaction with large amplitude in the wind direction is initially observed, which decreases due to soil dissipation.

In Figure 5, two-dimensional diagrams representing the movement of the central point of the roof during the aero-elastic simulation are presented as function of reduced wind velocity. Note that, before the coordination between the mechanical frequency of the structure and the vortex shedding, displacements are created in the direction of the wind. However, when the phenomenon of aero-elastic instability begins, due to the action of large vortices that separates from the lateral walls of the building, displacements created in the lateral direction. It can be seen that fluctuations occur mainly in wind direction at low velocity. As the wind speed increases, the displacement is mainly driven into the lateral wind direction, due to the effect of an asymmetric wake flow that is created from the separation from the side walls of the building.

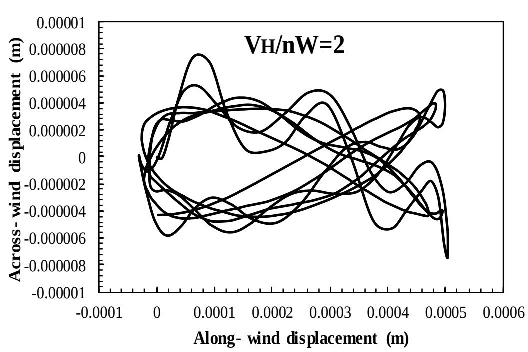

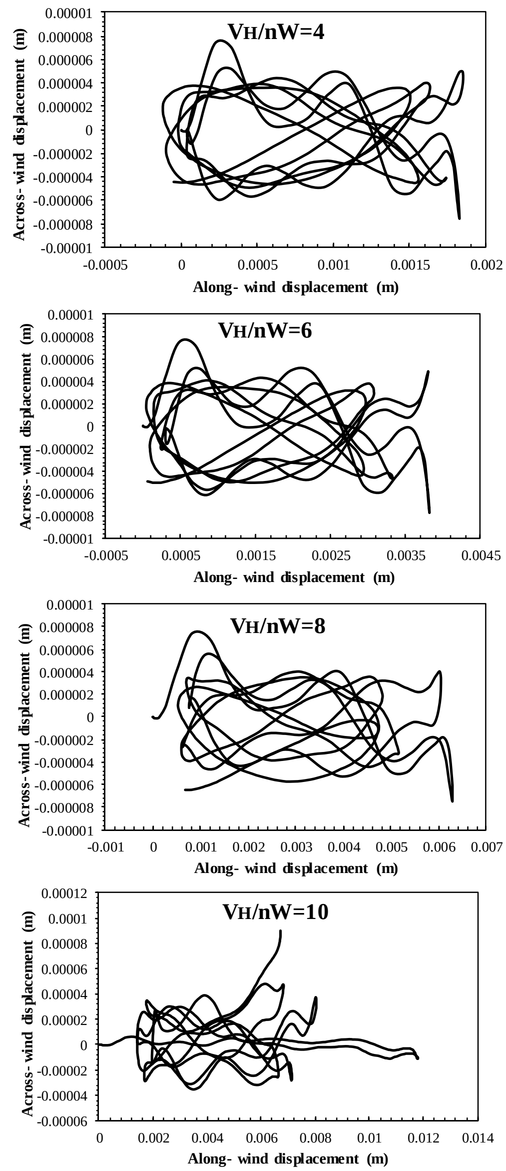

Figure 5. CAARC building top node path at five reduced speeds V_r =2,4,6,8 and 10 for CAARC building

6.1 Effect of plan shape

To investigate the effect of cross-sectional shape on the wind response of CAARC building described in the previous section, the series of analysis were carried out on a circular model with the same characteristics as the CAARC building. The displacement of the model at V_r=2 is positive but at other speeds is around zero and as time passes, amplitude increases. In addition, speed increase result in amplitude increase except at V_r=10. Longitudinal displacement curves are presented in Figure 6.

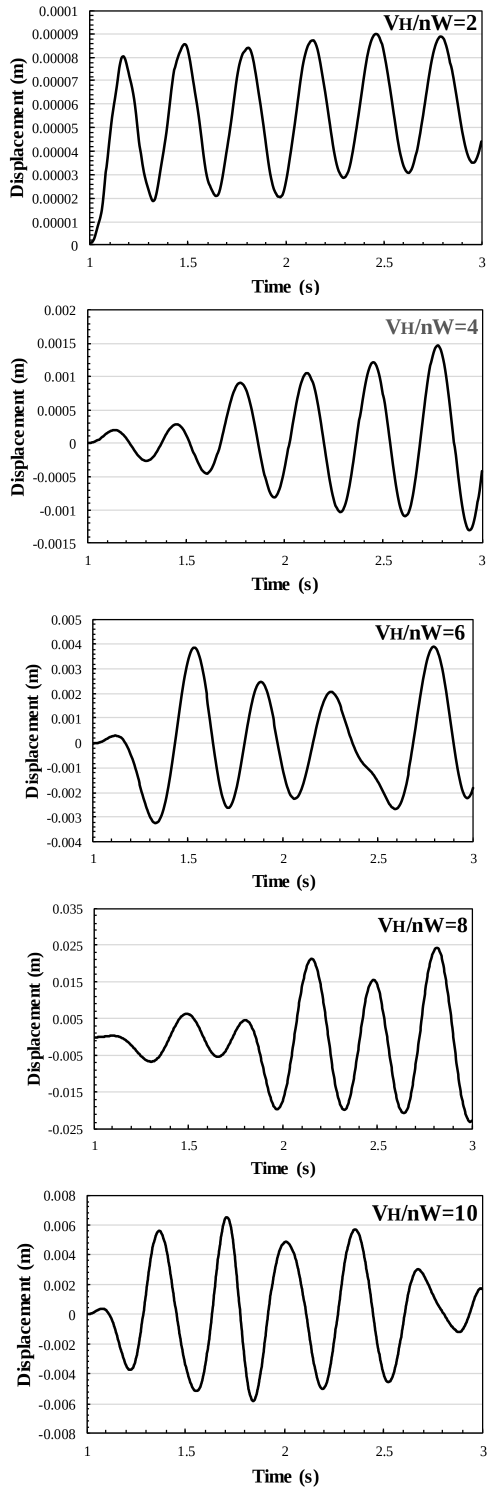

Figure 6. Time histories for along- wind displacements above the circular CAARC building for V_r= 2, 4, 6, 8 and 10

The statistical values of the building response have been calculated and are shown in Figure 7. Numerical results have been compared with numerical results related to the rectangular CAARC state. Here, the mean and r.m.s. of normalized displacement above the CAARC building in the longitudinal wind direction are shown. It can be seen that the mean normalized longitudinal wind responses obtained in the present simulation are very low in comparison with the rectangular state measurements and at a speed of V_r=4 and 6 are at lowest values. Inversely, r.m.s. of displacements are higher at the same values, but at the velocity of V_r=10 decreases.

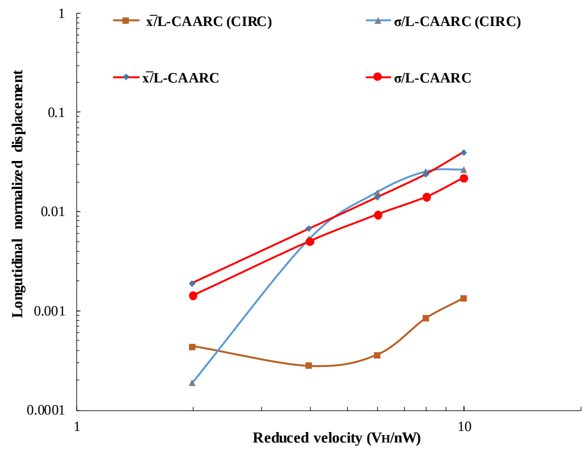

Figure 7. Normalized longitudinal displacements as a function of reduced velocity

Figure 8 shows the two-dimensional diagrams representing the path of the central point of the roof during the aero-elastic simulation for different wind speeds simulated in the aero-elastic analysis with structural damping. At V_H/nW= 2, the amplitude of displacements and its mean is slightly greater than zero. For the rest of the wind speeds, this trend change. As the velocity increases, the amplitude of displacements increases rapidly in both directions, while its average is around zero.

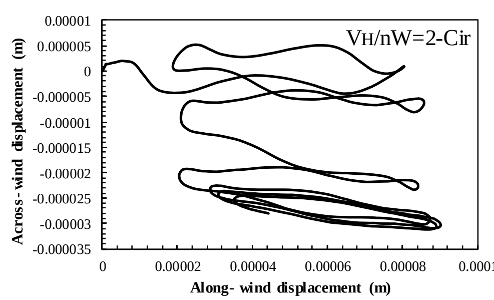

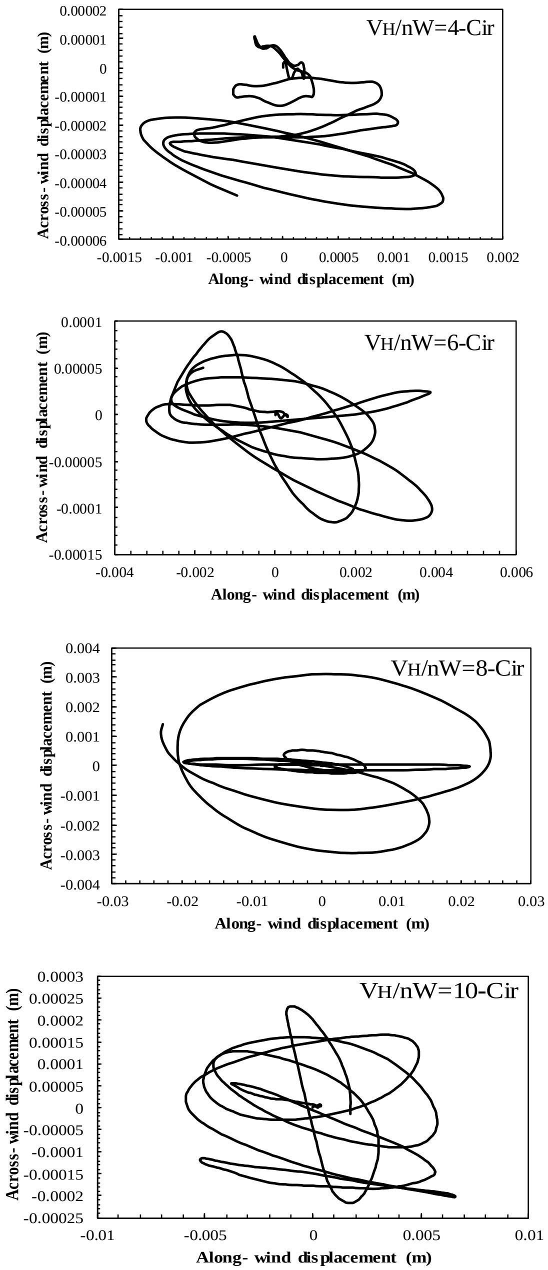

Figure 8. CAARC building top node path at five reduced speeds V_r =2,4,6,8 and10 for circular CAARC building

6.2 Effect of slenderness ratio

Also, to investigate the effect of slenderness in the wind response of CAARC building described in the previous section, a series of analysis was conducted on the building with half of the CAARC building height, while their other features were considered the same as CAARC building. The comparison between the normalized mean displacement $\bar{x}/L$ and normalized r.m.s. displacement σ_x/L above the CAARC building in longitudinal wind direction for these models in Figure 9 shows that are 20 times larger than short model state.

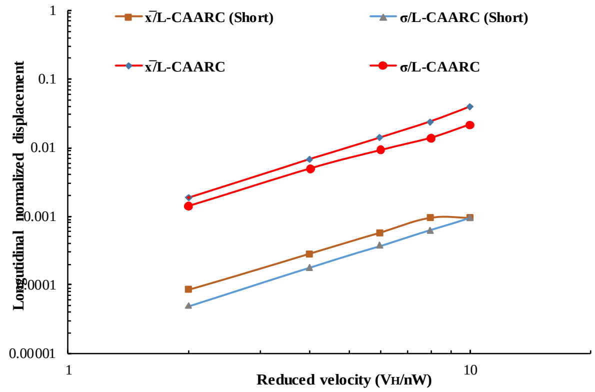

Figure 9. Longitudinal displacements as a function of reduced velocity

Figure 10 shows the different time histories of longitudinal displacements above the building for different wind speeds simulated in the aero-elastic analysis. As expected, the longitudinal displacement amplitude increases with increase of speed, which also is confirmed for the mean longitudinal displacement. For all of the wind velocities, the same trend is observed. The displacement amplitude and its average gradually decrease, except in the case of V_H/nW= 10 that mean value of displacement is nearly constant.

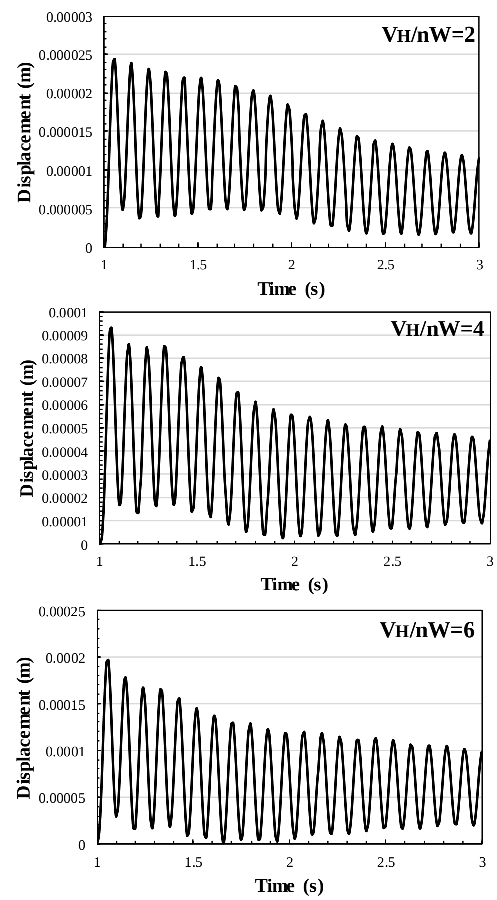

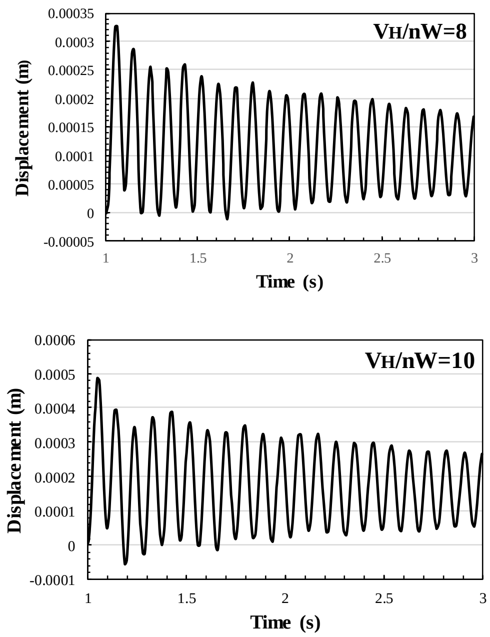

Figure 10. Time histories for along- wind displacements above the short CAARC building for V_r= 2, 4, 6, 8 and 10

Figure 11 shows two-dimensional diagrams that show the movement of the central point of the ceiling during the aero-elastic simulation for short CAARC state as the function of wind velocity. It can be seen that fluctuations are mainly at the wind direction at all wind speeds. As the wind speed increases, the displacements mainly occur in the direction of the wind direction rather than lateral direction. Since phenomenon of aero-elastic instability does not happen in this case so the amplitude of displacement is nearly constant.

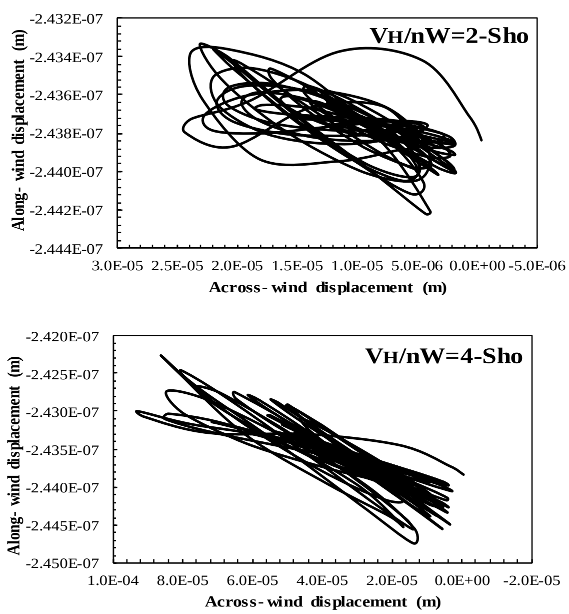

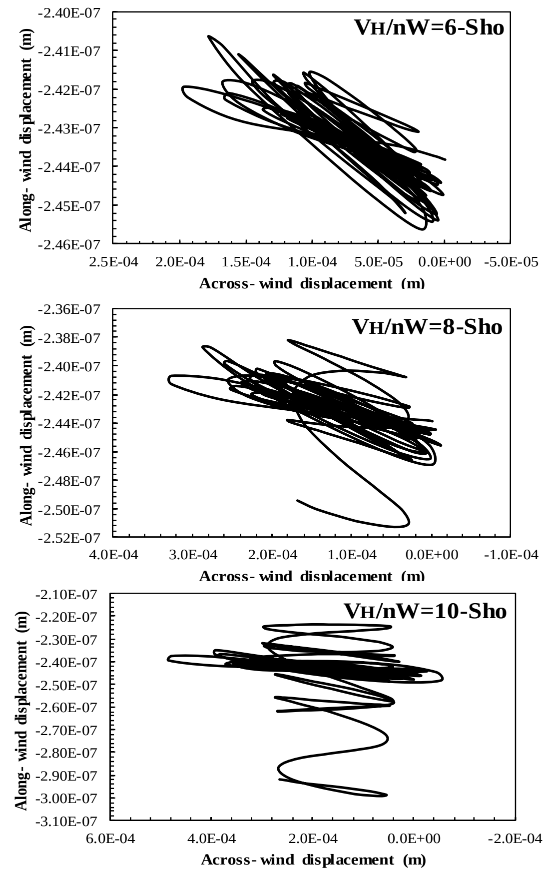

Figure 11. CAARC building top node path at five reduced speeds V_r =2,4,6,8 and10 for short CAARC building case

7. CONCLUSIONS

Some important remarks from the results of the numerical model proposed in this paper can be indicated as:

1- The mean normalized displacement in the wind direction ($\bar{x}/L$) for circular building that numerically evaluated without structural damping is considerably uncorrelated with CAARC building predictions. An agreement between the current results and the CAARC results in terms of normalized r.m.s. of wind displacements are significant (σ_x/L), although acceptable compliance is observed in upper limits of reduced velocity here. As expected, responses in short CAARC were resulted in underestimation of mean and r.m.s. in comparison with the corresponding measurements. Estimated r.m.s. of normalized displacements in the longitudinal wind direction (σ_x/L) are clearly 20 times smaller than CAARC measurements.

2- According to 2*D* plots, cross section has a significant impact on the prediction of the transverse displacement of buildings. Initially, when circular case considered, its amount increases, and in short case it decreases.

3- The effect of different plans on the structural response is significant in terms of along-wind displacements. The response obtained in circular case, in general, is characterized by displacements smaller than those in rectangular case. However, the decrease in top displacement along the longitudinal direction is relatively the same as the short model. The specific soil model that has been used has a significant impact in order to obtain real results.

References:

Zienkiewicz, O.C., R.L. Taylor. 1998. The Finite Element Method. Butterworth-Heinemann.

Wardlaw, RL., GF. Moss, 1970. A standard tall building model for the comparison of simulated natural winds in wind tunnels. CAARC, C.C.662m Tech; 25.

Melbourne, WH., 1980. Comparison of measurements on the CAARC standard tall building model in simulated model wind flows. *J Wind Eng Ind Aerodynamics*; 6(1–2), pp. 73–88.

Hirt, CW., JD. Ramshaw, LR. Stein, 1978. Numerical simulation of three-dimensional flow past bluff bodies. *Comput Methods Appl Mech En*g, 14(1), pp. 93–124.

Braun, A.L., A.M. Awruch, 2009. Aerodynamic and aeroelastic analyses on the CAARC standard tall building model using numerical simulation. *Comput. Struc*t., 87, pp. 564–581.

Huang, S., QS. Li, S. Xu, 2007. Numerical evaluation of wind effects on a tall steel building by CFD. *J Construct Steel Res*, 63:, pp. 612–27.

Stathopoulos, T., BA. Baskaran, 1990. Boundary treatment for the computation of three-dimensional wind flow conditions around a building. *J Wind Eng Ind Aerodynamics*, 35, pp. 177–200.

Harte, M., B. Basu, S. Nielsen, 2012. Dynamic analysis of wind turbines including soil- structure interaction. Eng Struct, 45, pp. 509–18.

Kausel, E., 2010. Early history of soil–structure interaction. *Soil Dyn Earthq Eng*., 30, pp. 822–32.

Halabian, AM., MH. El Naggar, 2002. Effect of non-linear soil–structure interaction on seismic response of tall slender structures. *Soil Dyn Earthq Eng*., 22, pp. 639–58.

Jeremic, B., G. Jie, M. Preisig, N. Tafazzoli, 2009. Time domain simulation of soil– foundation– structure interaction in non-uniform soils. *Earthq Eng Struct Dyn*; 38(5), pp. 699–718.

ABAQUS, 2012. ABAQUS Analysis User's Manual, Minneapolis, Minnesota, Dassault Systemes Simulia Corp., USA.

Felippa, CA., KC. Park, C. Farhat, 2001. Partitioned analysis of coupled mechanical systems. *Comput Methods Appl Mech Eng.*, 190, pp. 3247–70.

Zhang, Q., T. Hisada, 2004. Studies of the strong coupling and weak coupling methods in FSI analysis. *Int J Numer Methods Eng.*, 60, pp. 2013–29.

Borja, R.I., W.H. Wu, A.P. Amies and H.A. Smith, 1994. Nonlinear lateral, rocking and torsional vibration of rigid foundations, *J. Geotech. Eng.*, 120(3), pp. 491-513.

Matinmanesh, H. and M.S. Asheghabadi, 2011. Seismic analysis on soil-structure interaction of buildings over sandy soil, *Procedia Eng.*, 14, pp. 1713-1743.

Chu, D. and K.Z. Truman, 2004. Effects of pile foundation configurations in seismic soil-pile-structure interaction, *13th World Conference on Earthquake Engineering*, Vancouver, B.C., Canada.